

Shallow water 3D CSEM: A case study from Malaysia

Håkon Toralv Pedersen*, EMGS ASA, M. Akmal Affendi B. Adnan, Azani B. A. Manaf, Petronas

Summary

CSEM has been perceived as a deep water technology due to strong airwave interference in shallow waters. Recent developments, in particular 2.5D and 3D anisotropic inversion schemes and frequency differencing, are now capable to better cope with the additional complexity of the measured data in shallow waters. In this case study, we present the results of a 3D CSEM survey acquired in ~90m water depth and discuss the benefits and disadvantages of available interpretation tools including attribute analysis and inversion. A clear high resistivity feature is mapped within each of the seismic prospects at target depth. Consequently, the results of the CSEM survey decreased the geological risk of the two prospects for the oil company.

Introduction

Subsurface resistivity imaging of shallow water Controlled Source ElectroMagnetic (CSEM) data has been considered difficult due to strong effects of the refracted and reflected energy from the sea-surface, commonly referred to as the airwave. The airwave will dominate the measured response, effectively masking the subsurface response. The phase of the inline electric field measured by a receiver in 90m water depth is shown in Figure 1, illustrating the strong airwave behavior from 5000m offset onwards. The airwave induces horizontal currents (Constable and Weiss, 2006) similar to naturally occurring magnetotelluric fields. In the presence of electrical anisotropy, an isotropic inversion will therefore not capture the complexity in the observed data, rendering the reconstructed resistivity distribution of the subsurface non-quantitative and uncertain. Recent developments in processing and inversion algorithms have provided a solid platform for better interpretation and imaging of shallow water CSEM data through anisotropic inversion schemes and frequency differencing (Maaø and Nguyen, 2009). In this case study we will present results from a shallow water survey (~90m water depth) in Malaysia acquired in 2008. We will compare the recently developed inversion methods to more simplistic processing and analysis tools and discuss their benefits and disadvantages. All inversion results presented have data misfit less than 10%.

Survey area

The survey layout and prospect outlines are shown in Figure 2. A total of 90 receivers were deployed in two grids, thus recording inline and wide azimuth data. In addition, a line of 9 receivers was added in the N-S

direction for delineation purposes of the SW prospect. The SW prospect is a 4-way dip closure and the NE prospect is a 3-way dip closure with a vertical column of 35 meter for both structures. The prospects are 12 km apart and the areal extents are approximately 27km² and 12km² for the SW and NE prospect, respectively. The SW prospect has a strong reflector below the crest of the structure, highlighted in Figure 3, believed to be related to hydrocarbon (gas) accumulation. The reservoir rock is Late-Middle Miocene to Late Miocene sands. Nearby wells yield good results for hydrocarbon presence in the Late-Middle Miocene to Late Miocene section. The transgressive upper bathyal shale of Early to Middle Pliocene provides a good top seal while Late-Middle Miocene to Late Miocene intra-formational shale acts as a lateral seal. A matured source from Early-Middle Miocene coastal plain to coastal is expected to charge the prospects situated in surrounding areas. The hydrocarbon migration is considered close to the source due to a possible kitchen area located 20 kilometer away from these prospects.

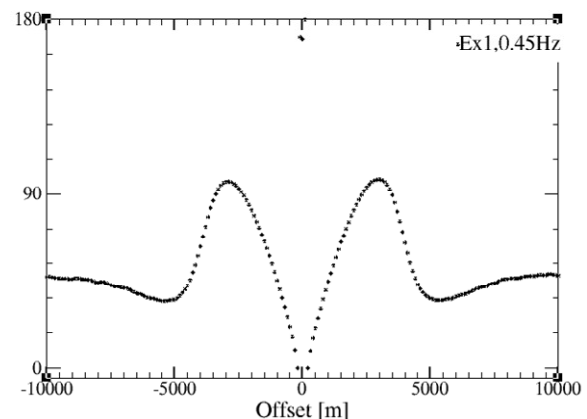


Figure 1: Phase versus Offset (PvO) of the inline electric field at 0.45Hz measured in 90m water depth. The airwave is dominating the response from 5000m offset onwards.

Attribute analysis

A first overview of the resistivity distribution can be obtained by an attribute analysis. The airwave effects are reduced by decomposing the EM field measured at the seabed into up-going and down-going components and removing the latter (Amundsen et al., 2006). This processing step is done before the attribute generation, namely Normalized Magnitude versus Offset (NMvO) and Phase Difference versus Offset (PDvO). These attributes

Shallow water 3D CSEM

are limited to a qualitative assessment, stating that one area is more resistive than the other. Figure 2 shows the results of the areal NMvO at 4500m offset, an offset sufficiently large for the EM field to travel down to and beyond the target depth. Indications of lateral coincidence between the seismic prospect and the EM anomalous areas can be observed, but the analysis is inconclusive. The phase and magnitude attributes are conformable.

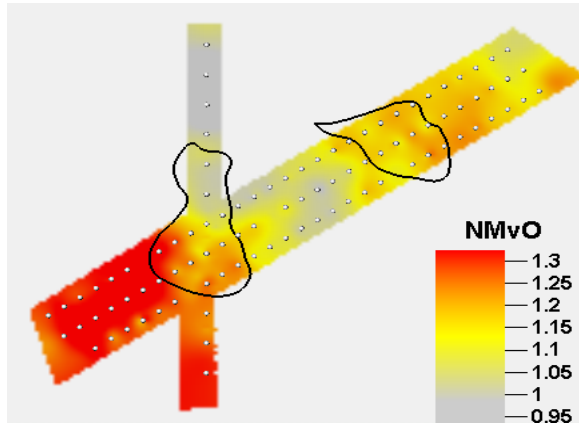


Figure 2: Survey layout with receivers (grey spheres) and seismic prospects (black polygons). Areal Normalized Magnitude versus Offset (NMvO) at 4500m offset, 0.45Hz, displayed in colors.

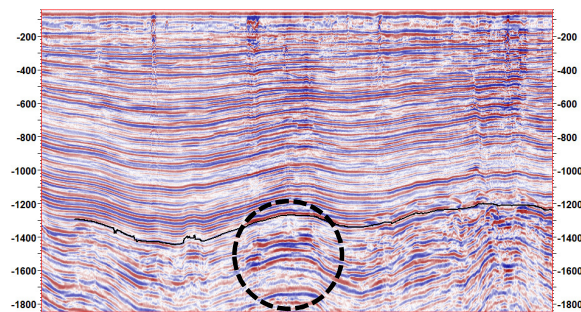


Figure 3: Seismic cross-section across the SW prospect. The structure and high amplitude event are highlighted by the dashed circle.

Anisotropic 2.5D inversion

2.5D inversion is the first step in the quantitative data analysis; 2.5D meaning that the electromagnetic field is modeled in 3D but assuming a 2D resistivity model, i.e. the resistivity is presumed to be invariant orthogonal to the source towing direction. Anisotropic 2.5D inversions were used to get a first impression of the resistivity distribution and possible burial depths of the anomalous areas observed in the attributes. An adjacent well north of the survey area

served as a calibration point for the horizontal resistivity profile resulting from the inversions. Figure 4 shows two clear distinct resistive features for the middle W-E line starting at target level which are laterally well delineated and in compliance with the seismic prospects. In addition, the S-N line was inverted to test if the SW prospect would yield similar results independent of towing direction, which was confirmed. The resistivity distribution of the background, i.e. outside of the target area, at the source towline crossing has converged to a comparable model, increasing the confidence in the two inversion results. No seismic information (Hansen and Mittet, 2009) was used to constrain these inversions.

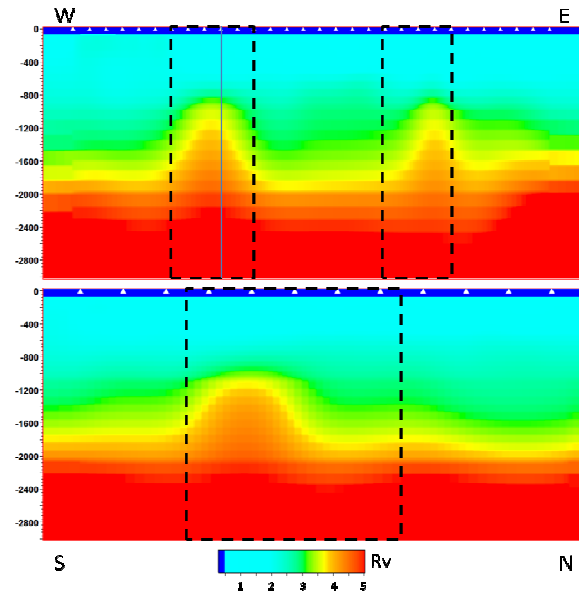


Figure 4: Vertical resistivity (R_v) distribution from anisotropic 2.5D inversions. Dashed lines are prospect outlines, solid line is the line crossing and white triangles are receiver positions. Upper image: Middle West-East line. Lower image: South-North line.

Even though 2.5D inversion has proven to be a robust inversion scheme, it has its limitations. The assumption of invariant resistivity in the cross-line direction renders 3D effects unresolved. This will be discussed in more detail in the discussion section below. In addition, broadside source data is provided by the azimuth data. The complementary information in the inline and broadside data yields better determination of the vertical position of a resistive body (Morten et al., 2009). The two distinct separate features are continuous from approx 1200 meters below sea level down into higher resistive strata. To investigate the possibility of an inversion “smearing” effect, an anisotropic 3D inversion was performed.

Shallow water 3D CSEM

Anisotropic 3D inversion

The survey area was divided into two separate grids to reduce the processing time of each of the inversion runs and the S-N line was excluded. The details of the inversion scheme used are presented by Zach (2008). The start model for the 3D inversion was built using interpolation of resistivity profiles picked from lower dimensional inversion results, namely CMP and 2.5D inversions. This provided a start model that captured the background trends observed by the CSEM data and the in-situ resistivity measurements of an adjacent well to the North. Figure 5 shows the result of the anisotropic 3D inversion for the SW prospect. We observe that the spatial placement of the resistive body is in compliance with the seismic prospect. Figure 6 shows the anisotropic 3D inversion result for the NE prospect. The spatial positioning of the high resistive feature shows good agreement between CSEM and seismic.

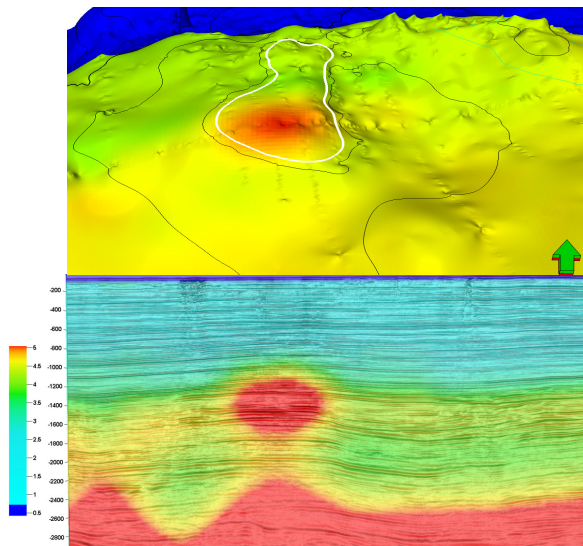


Figure 5: Vertical resistivity (R_v) distribution from anisotropic 3D inversion of the SW prospect. The same color scale is used for both images. Upper image: Extracted R_v along the top of the reservoir. Lower image: R_v superimposed to seismic.

Discussion

Attribute analysis can be a powerful tool to identify local resistors from deep water CSEM data. However, in shallow water environments the airwave will mask the subsurface response, rendering this processing step too simplistic. Reducing the airwave effect is required in order to extract subsurface information, in this case study obtained by up-down wave field decomposition. Although proven

effective, this method has limitations since it assumes that the recorded fields consist of purely vertically travelling wave fields.

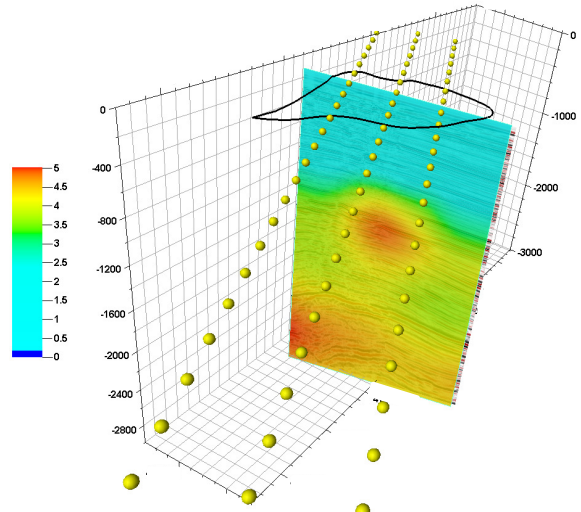


Figure 6: Vertical resistivity (R_v) distribution from anisotropic 3D inversion of the NE prospect superimposed to seismic. Yellow spheres are receiver positions and the black polygon is the prospect outline.

In addition, the limitation of attributes becomes clear when one encounters varying anisotropy in a survey area. Such variations can cause anomalous responses, as illustrated by a simple 1D modeling example shown in Figure 7, which require attention if the target is predicted to be characterized by a low resistivity contrast. One can also observe that the “anisotropy anomaly” can be offset dependent. If the expected detection offset for a target falls within the anisotropy anomaly offset interval, this must be considered in the attribute interpretation.

To quantify the subsurface resistivity in shallow waters it is paramount to account for the airwave in the data. If the airwave is modeled inaccurately, the inversion may compensate for the modeling inaccuracy by introducing resistivity artifacts. In CSEM measurements with strongly varying bathymetry, where one expects varying conductivity profiles orthogonal to a source towline, the invariance assumption of the 2.5D inversion could potentially be a source of modeling error. However, the seabed topography in the survey area for this case study is smooth with only minor water depth variations, so the airwave is assumed to be modeled correctly by the 2.5D forward operator. In the 3D inversion, the airwave is also modeled in 3D, but considers conductivity measurements of the water column along all towlines, thus providing

Shallow water 3D CSEM

higher confidence in the resulting subsurface resistivity distribution. More importantly, since the airwave induces horizontal currents in the subsurface, shallow water isotropic inversions may not capture the complexities in the data resulting from anisotropy. The local resistors observed in the anisotropic 2.5D inversions were not reconstructed by isotropic 2.5D inversion runs, demonstrating the above mentioned.

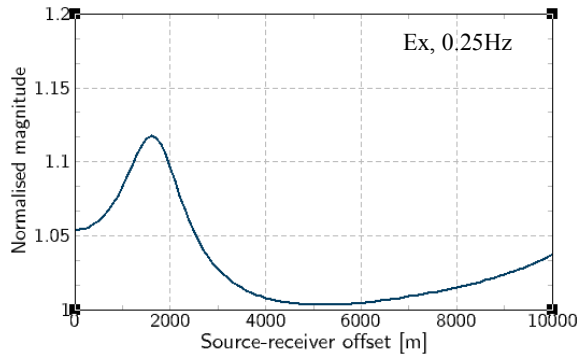


Figure 7: The in-line electric field of a 1D anisotropic model (2000m water depth, halfspace $1.5\Omega\text{m}$ vertical resistivity and $1\Omega\text{m}$ horizontal resistivity) normalized against the response of a corresponding 1D isotropic model (2000m water depth and $1.5\Omega\text{m}$ halfspace).

Even though the anisotropic 2.5D inversion identified two local resistors, it also has limitations. Firstly, the vertical resolution is reduced compared to 3D inversion which includes azimuth data. The vertical resolution limitation is reflected in the inversion results in Figure 4. The local resistive features at the target depth are continuous down to higher resistive strata and this continuity is not expected by the current geological knowledge nor is it observed outside the prospects. Secondly, the assumption of infinite target extent orthogonal to the source towline can cause misinterpretations as a result of unresolved 3D geometry effects. The effect of reducing a target from having an infinite width to having a width of 2km is illustrated qualitatively by a simple modeling exercise in Figure 8. When the width is reduced, lower NMvO is observed for the in-line electric field. In other words, lower resistivity is required to explain the data with an infinite target width, assuming that the target length along the towing direction is kept constant. This could be the cause of the relatively low resistivity imaged at target depth, since the extent of the prospect is limited to 27km^2 and 12km^2 , respectively.

The limitations of attribute analysis and 2.5D inversion are addressed by an anisotropic 3D inversion. Azimuth data is included, providing the broadside source data which is very sensitive to the horizontal resistivity. The reconstructed horizontal resistivity from the anisotropic 3D inversion was

comparable to the resistivity log of the adjacent well. The resistive features are separated from the deeper strata in compliance with current geological understanding of the area. The relative low resistivity contrast observed in the anisotropic 3D inversion result is a combined consequence of the low sensitivity of the inline data to target thickness and the decoupling of the sensitivity to the vertical and horizontal resistivity in inline and broadside source data. A solution to this is to apply a priori anisotropy regularization (J.P. Morten, personal communication, 2010), but this has not been applied here. Nevertheless, the resistivity required to explain the data along the middle W-E line is a bulk measurement of $\sim 600\text{m}$ with $5\Omega\text{m}$ for the SW prospect. Transferring this bulk measurement to a 30m target thickness would be the equivalent of $\sim 100\Omega\text{m}$. Post-inversion 3D modeling is on-going to find a probable volume estimate. These CSEM results were included in the risk mitigation of the prospects and consequently lowered their risk.

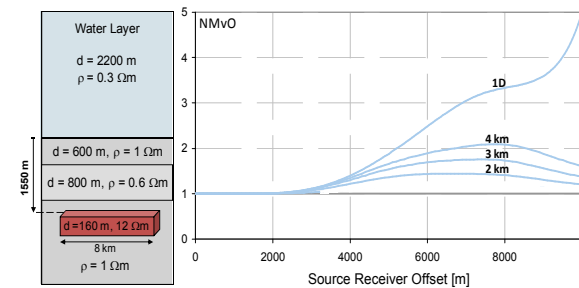


Figure 8: NMvO curves for the in-line electric field at 0.25Hz. The responses for models including a resistor with varying width are normalized against a reference case where the resistor is replaced by the background resistivity of $1\Omega\text{m}$.

Acknowledgements

EMGS would like to thank PETRONAS for the permission to show these results. The authors would like to thank Anh Kiet Nguyen and Lars Lorenz for the 3D and 2.5D inversion results, respectively. In addition, the authors would like to thank Siti Hassulaini Abdul Rahman for her sustained work on this data set.

EDITED REFERENCES

Note: This reference list is a copy-edited version of the reference list submitted by the author. Reference lists for the 2010 SEG Technical Program Expanded Abstracts have been copy edited so that references provided with the online metadata for each paper will achieve a high degree of linking to cited sources that appear on the Web.

REFERENCES

- Amundsen, L., L. Løseth, R. Mittet, S. Ellingsrud, and B. Ursin, 2006, Decomposition of electromagnetic fields into upgoing and downgoing components: *Geophysics*, **71**, G211–G223.
[doi:10.1190/1.2245468](https://doi.org/10.1190/1.2245468)
- Constable, S., and C. J. Weiss, 2006, Mapping thin resistors and hydrocarbons with marine EM methods: Insights from 1D modeling: *Geophysics*, **71**, no. 2, G43–G51, [doi:10.1190/1.2187748](https://doi.org/10.1190/1.2187748).
- Hansen, K. R., and R. Mittet, 2009, Incorporating seismic horizons in inversion of CSEM data: 79th Annual International Meeting, SEG, 694-698
- Maaø, F., and A. K. Nguyen, 2009, Enhanced subsurface response for marine CSEM surveying: 79th Annual International Meeting, SEG, 810-814
- Morten, J. P., A. K. Bjørke, T. Støren, E. Coward, S. A. Karlsen, and F. Roth, 2009, Importance of azimuth data for 3D inversion of Marine CSEM scanning data: 71st EAGE Conference and Exhibition
- Zach, J. J., A. K. Bjørke, T. Støren, and F. Maaø, 2008, 3D inversion of marine CSEM data using a fast finite-difference time-domain forward code and approximate hessian-based optimization: 78th Annual International Meeting, SEG, 614-618